

FIG. 1. Mean relative dominance of the sapling layer ($> 2 \text{ m}$, $< 10 \text{ cm dbh}$) for the seven most common tree species and all other canopy and subcanopy tree species combined in salvaged areas with scarification, salvaged areas without scarification, and controls at the onset of the study (2004) and 5 yr post-salvaging (2011).

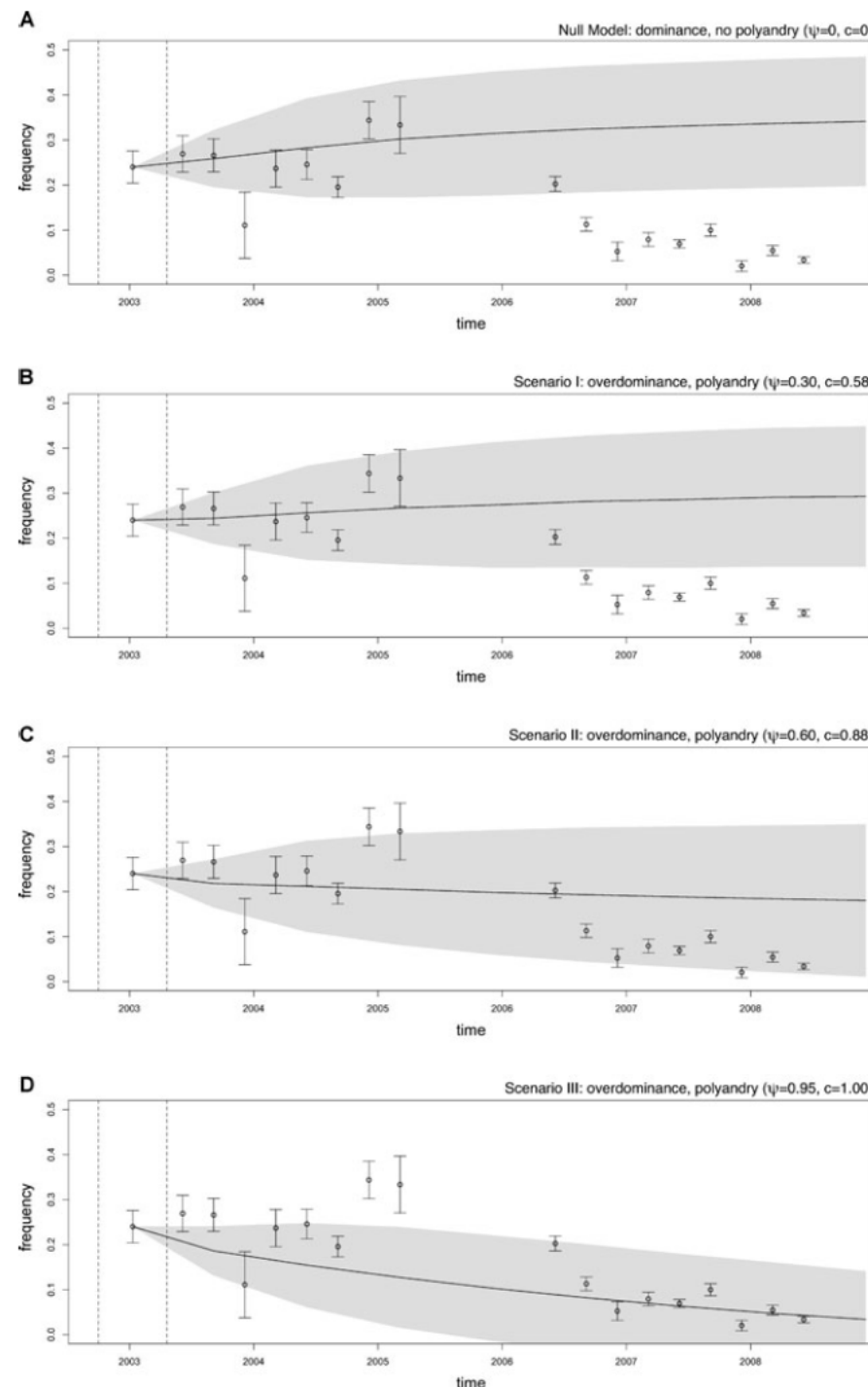
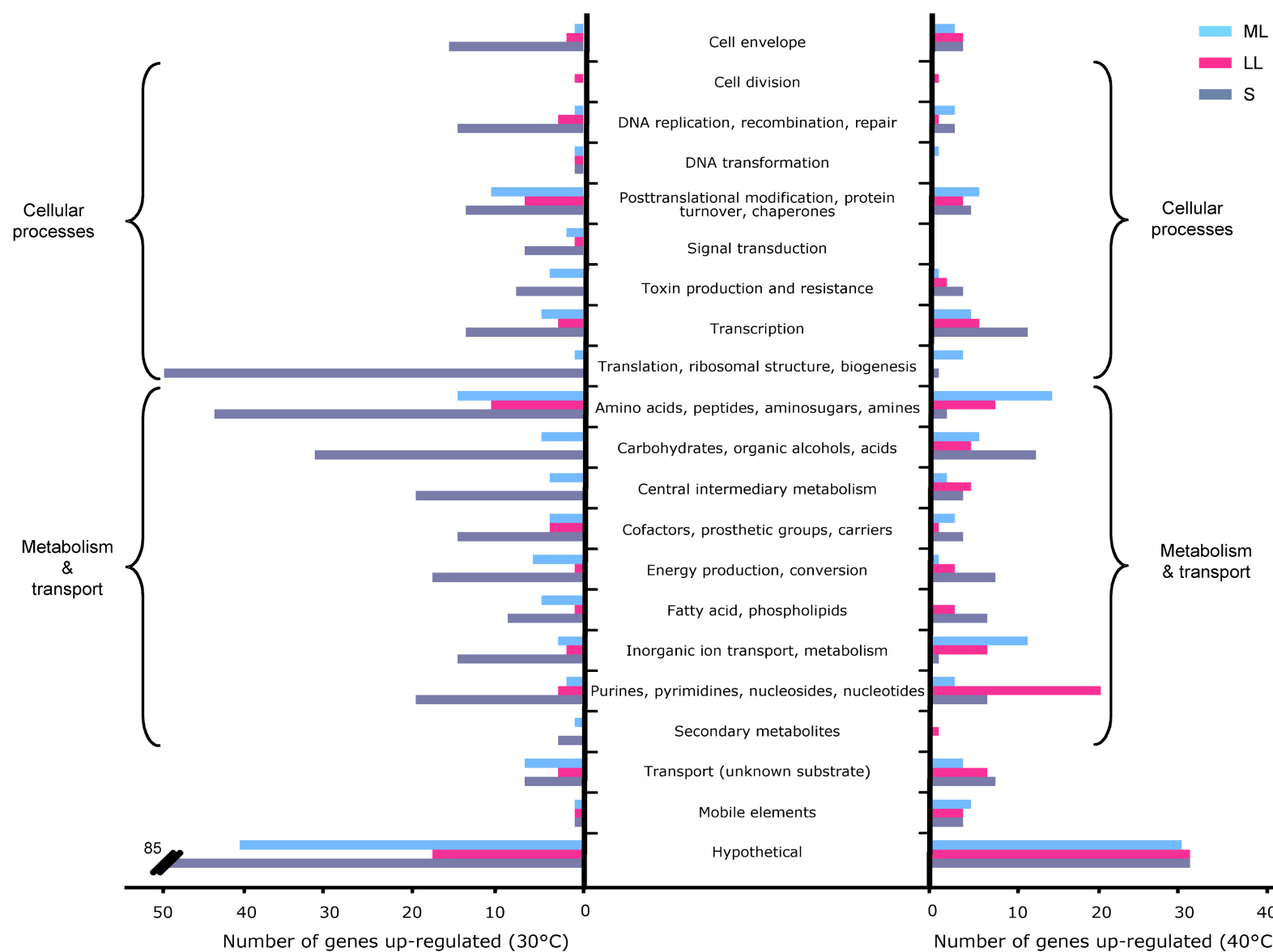
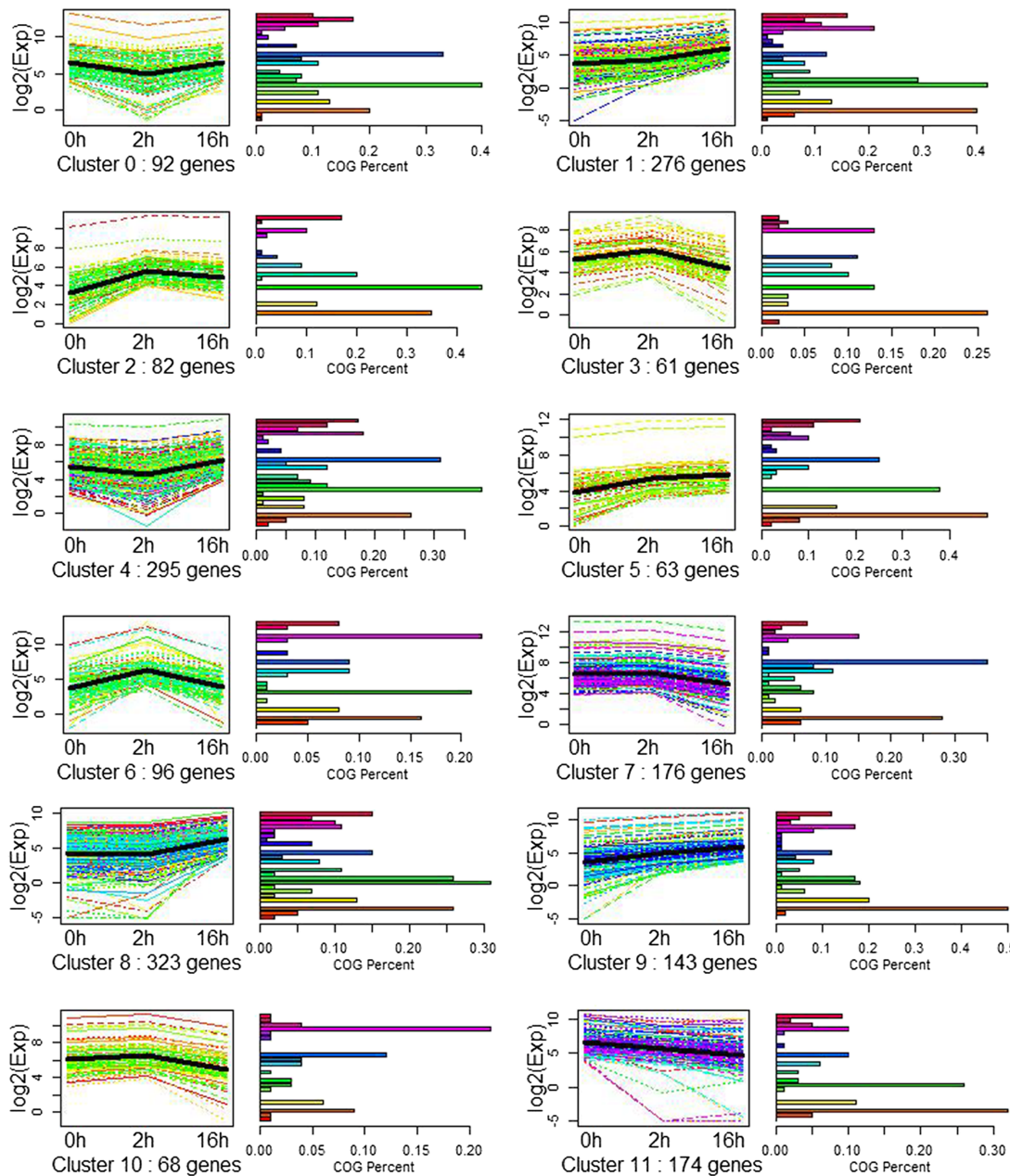


Figure 2. Observations from the wild population and simulation predictions from October 2002 until June 2008. The red dot represents the initial t frequency among the first 50 adults \pm SE. Each black dot represents the t frequency among the pups born in the given 3-month time interval \pm SE ($n_{\text{tot}} = 2177$). Gray and red lines show model predictions with 95% confidence intervals (shadows) for (A) the null model (dominance and no polyandry) and (B)-(D) scenarios I-III (in Table 3, overdominance and different levels of polyandry).

Figure 4. Differential regulation of gene expression in GBS strain NEM316 at 30°C and 40°C. Vanessa
Genes were classified into 21 main functional categories. Bars indicate the numbers of genes up-regulated at one
temperature in mid-logarithmic (ML), late logarithmic (LL), and stationary (S) phase.



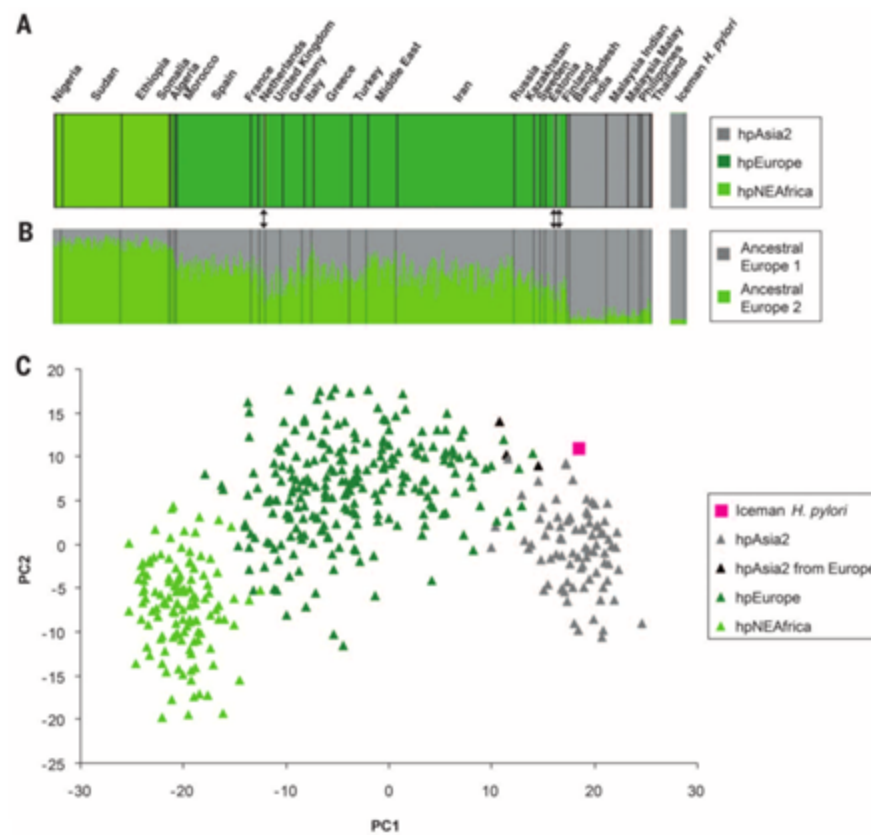


Wang J, Yang Y, Liu X, Huang J, Wang Q, Gu J, et al. Transcriptome profiling of the cold response and signalling pathways in *Lilium lancifolium*. BMC Genomics. 2014; 15: 203.
doi: 10.1186/1471-2164-15-203

Figure 4

SOM cluster analysis of gene expression in the 12 different patterns. Clusters were obtained by the k-means method on the gene expression profiles of the 1849 modulated genes. The most abundant group is Cluster 8 and 1, with 323 and 276 genes whose expressions show positive slopes during stage of T2h to T16h embryogenesis. The second abundant group is Cluster 4, which contained 295 genes whose expression shows a negative slope from C0h to T2h.

Fig. 3. Multilocus sequence analyses. (A) Bayesian cluster analysis performed in STRUCTURE displays the population partitioning of hpEurope, hpAsia2, and hpNEAfrica and the Iceman's *H. pylori* strain (details about the worldwide population partitioning of 1603 reference *H. pylori* strains are available in fig. S14). (B) STRUCTURE linkage model analysis showing the proportion of Ancestral Europe 1 (from Central Asia) and Ancestral Europe 2 (from northeast Africa) nucleotides among strains assigned to populations hpNEAfrica, hpEurope, and hpAsia2 and the Iceman's *H. pylori* strain on the extreme right. The black arrows indicate the position of the three extant European hpAsia2 strains. (C) Principal component analysis of contemporary hpNEAfrica, hpEurope, and hpAsia2 strains and the Iceman's *H. pylori* strain.



Guillaume

Good Picture

H3K36ac Is an Evolutionary Conserved Plant Histone Modification That Marks Active Genes^{1[OPEN]}

Walid Mahrez, Minerva Susana Trejo Arellano, Jordi Moreno-Romero, Miyuki Nakamura, Huan Shu,
Paolo Nanni, Claudia Köhler, Wilhelm Gruissem, and Lars Hennig*

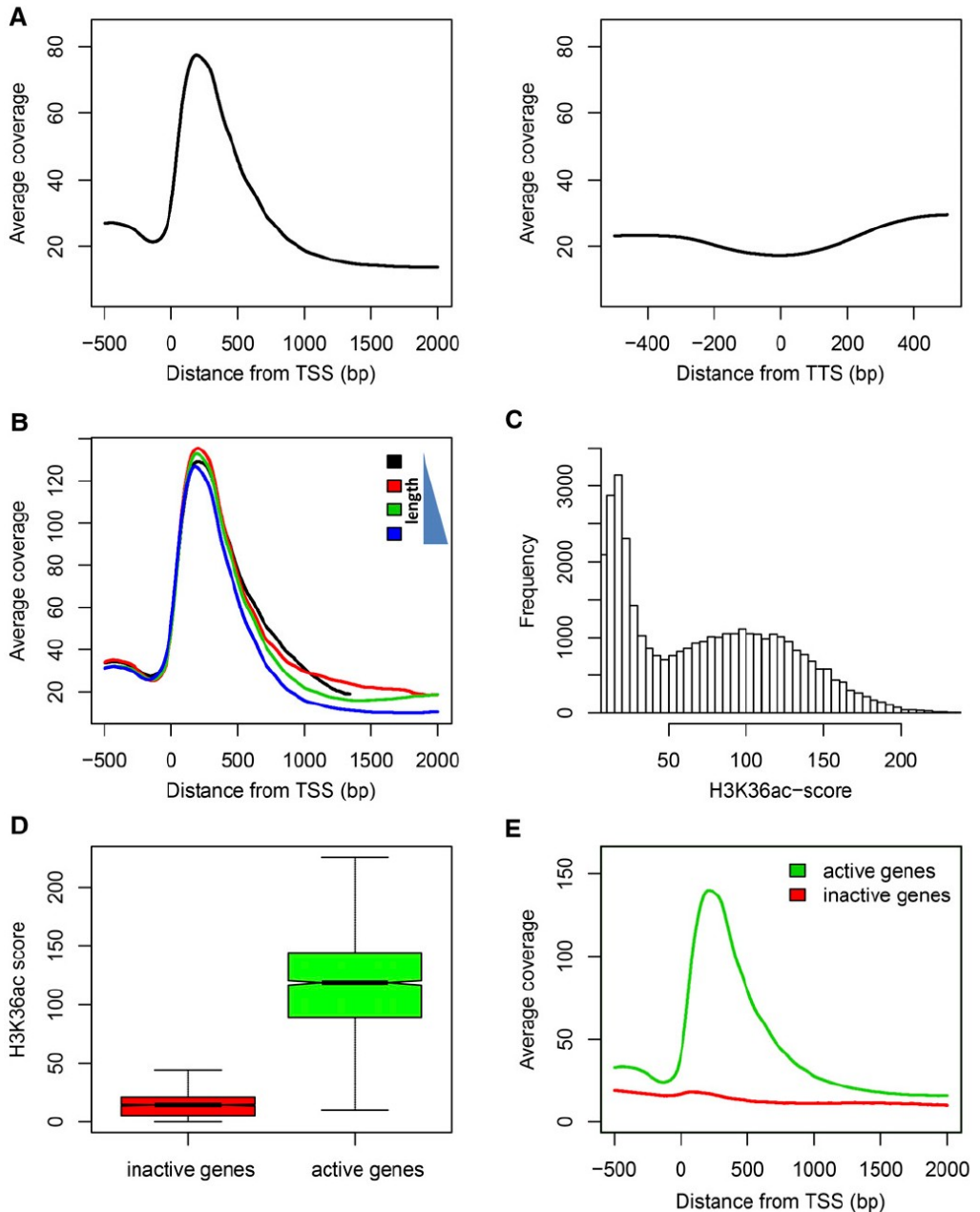
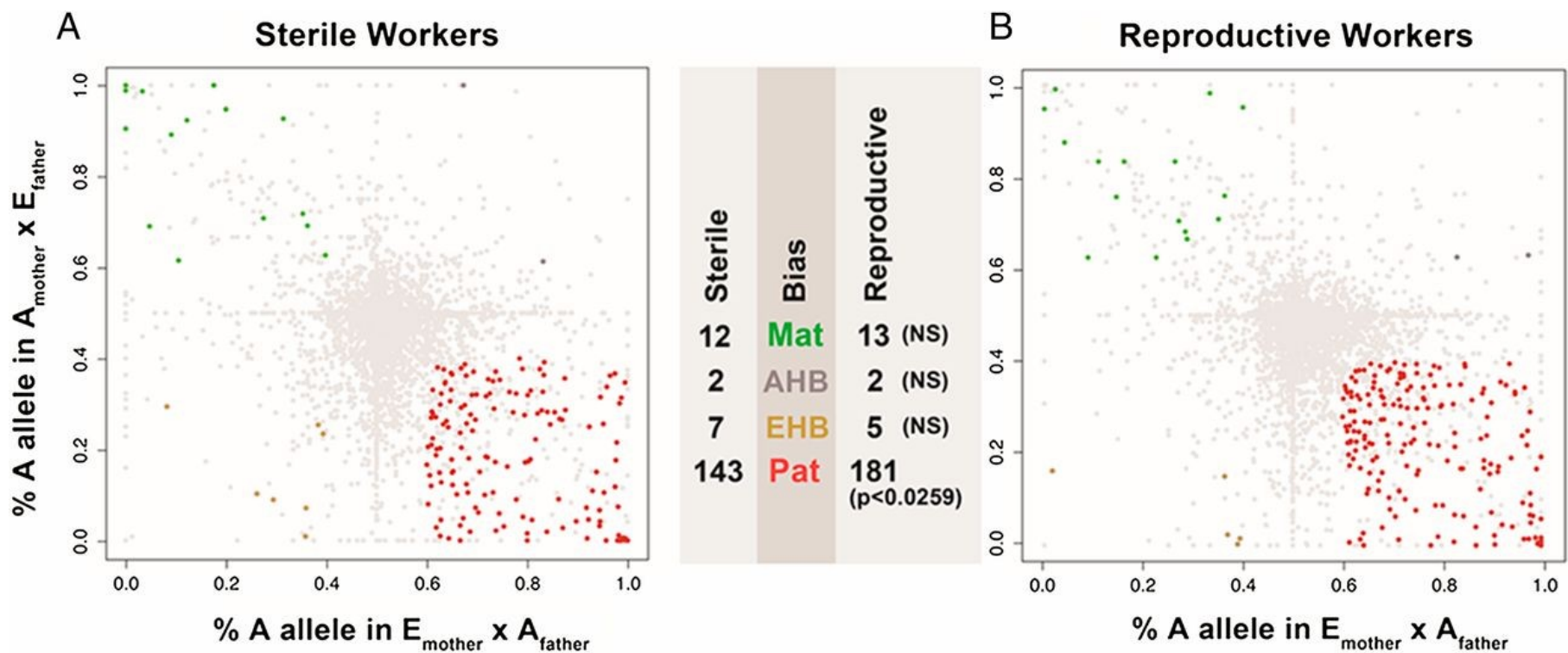
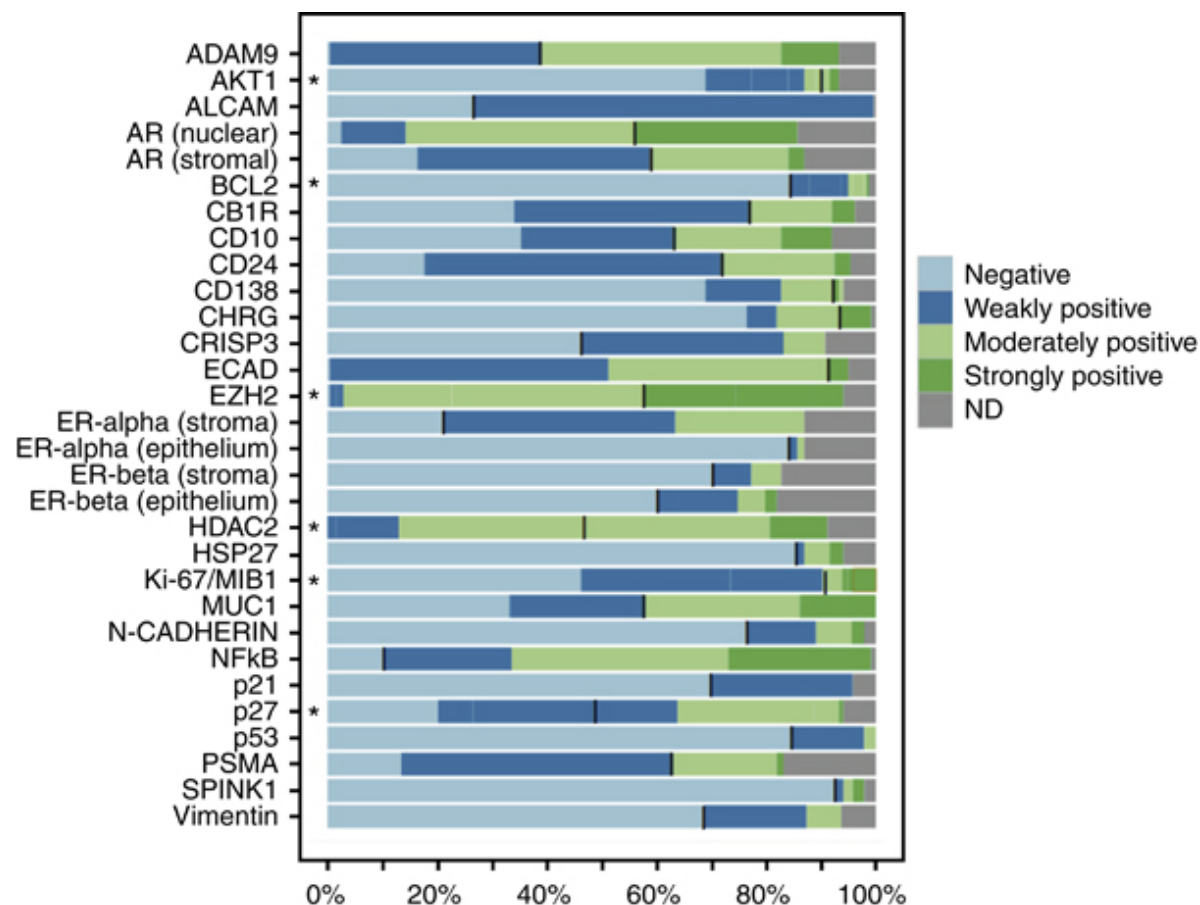


Figure 3. H3K36ac distribution across genes. A, Metagene plots of H3K36ac enrichment around the TSS (left panel) and (right panel). The highest enrichment was detected within the first 500 bp distal to the TSS. B, H3K36ac enrichment is independent of gene length. Metagene plots are shown for the first (black), second (red), third (green), and forth (blue) length quartile where black line represents the 25% shortest genes. C, Distribution of gene-specific H3K36ac scores defined as the mean H3K36ac signal within a window of 35 to 516 bp distal to the TSS. Note the two separate populations of genes with scores of less or more than 27, respectively. D, Relation between H3K36ac score and transcriptional state. H3K36ac scores are shown for the 10% genes with lowest (red) and highest (green) mRNA levels, respectively. E, H3K36ac metagene plot around the TSS for the 10% genes' lowest (red) and highest (green) mRNA levels, respectively. Only active genes have the characteristic H3K36ac peak within first 500 bp. Expression data are from Shu et al. (2012).

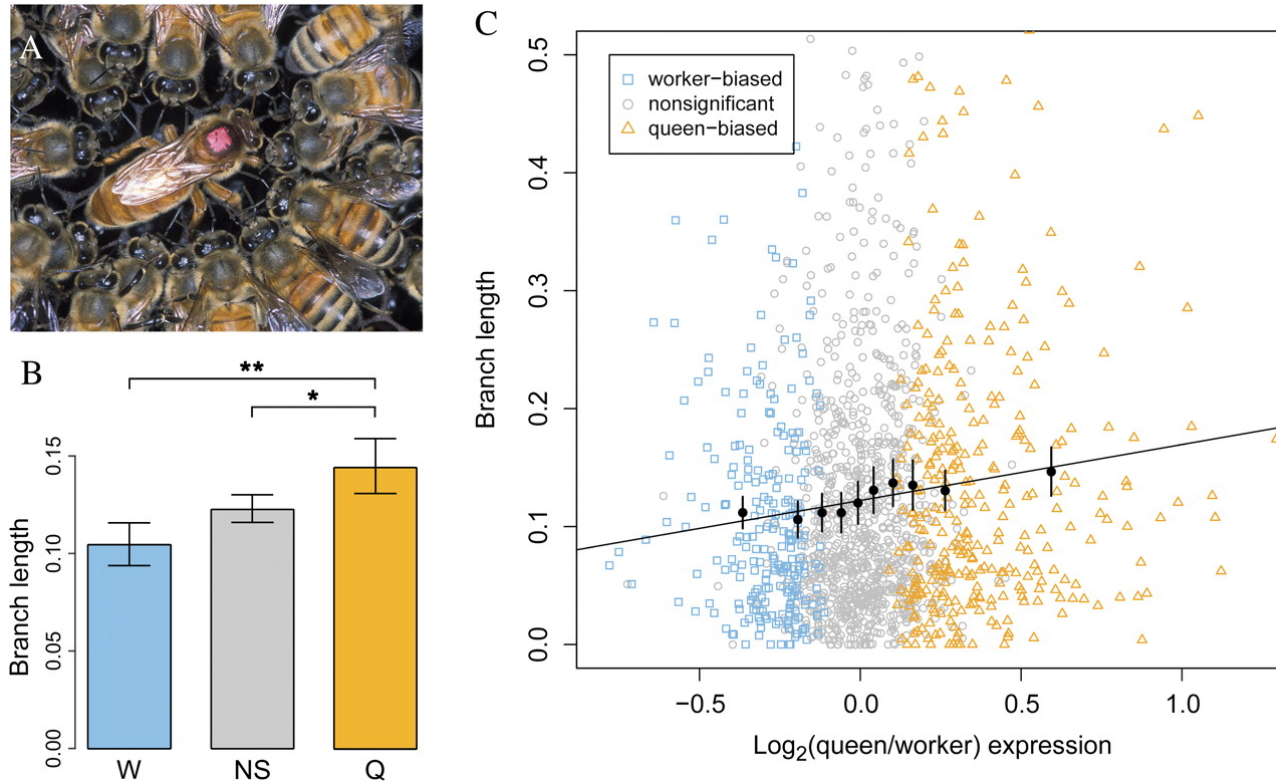


David A. Galbraith et al. PNAS 2016;113:1020-1025



Frequencies of immunohistochemically detected expression of selected prognostic markers in primary prostate carcinomas.

Markers labelled with an asterisk were recorded as immunoreactive scores and summarised for easier visualisation (IRS 0: negative, IRS 1–3: weakly positive, IRS 4–8 moderately positive, IRS>8: strongly positive). Black bars indicate the cut-off used for dichotomising the variable for Cox regression analysis. Abbreviation: ND: non determined/missing data



Caste-biased gene expression is linked to protein evolutionary rate in *Apis mellifera*.

(A) *Apis mellifera* workers surround a queen. (B) *Apis mellifera* evolutionary rates (branch lengths in amino acid substitutions per site) differ significantly among genes with worker-biased expression (W), nonsignificant bias (NS), and queen-biased expression (Q; Kruskal–Wallis $P = 0.0019$). Means with 95% confidence intervals are plotted, and significant differences are indicated ($*P < 0.05$ and $**P < 0.01$ pairwise Mann–Whitney U test with Bonferroni correction). (C) Log₂-transformed ratios of queen-to-worker gene expression are correlated with *A. mellifera* evolutionary rates (Spearman's rank correlation $rs = 0.096$, $P = 0.0002$). A linear model best-fit line is plotted, and mean values for 10 equally sized bins of genes are shown as black dots with 95% confidence intervals. Outliers beyond the scaled axes contribute to plotted means and confidence intervals.

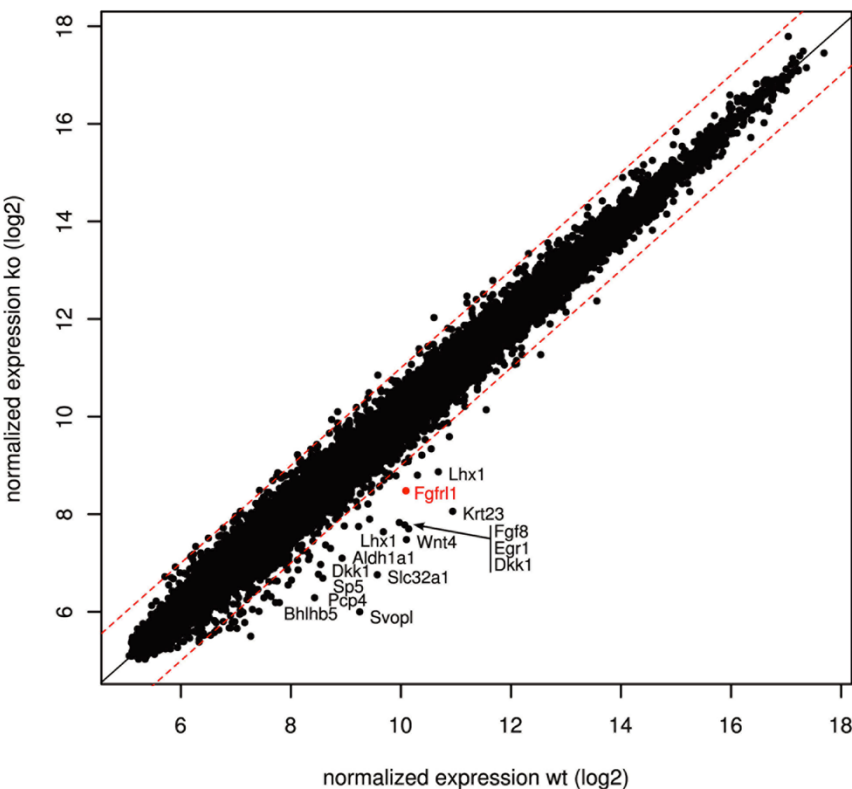
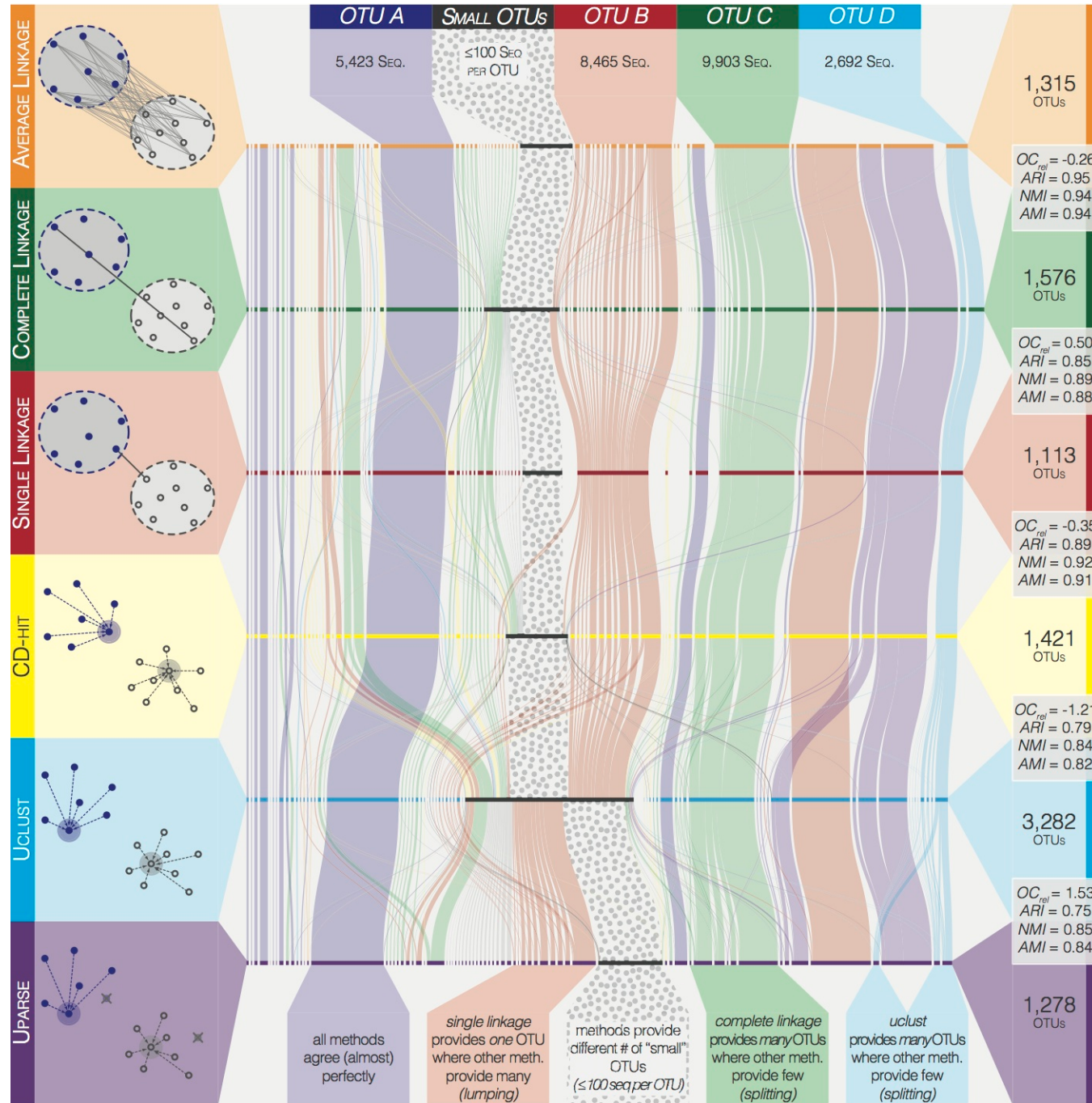


Figure 2. Identification of transcripts that are differentially expressed in *Fgfrl1* deficient kidneys.
The scatter plot shows average normalized signal intensities from three independent experiments using E12.5 kidneys from wildtype and *Fgfrl1* knock-out mice. Each dot represents an individual gene. Dashed lines correspond to a fold change of 2. Transcripts that are down-regulated more than 3-fold are given by their gene symbol.
<http://dx.doi.org/10.1371/journal.pone.0033457.g002>

Sebastian



Sebastian

